

The Survival of Planetary Nebulae in the Intracluster Medium

Eva Villaver¹

*Space Telescope Science Institute, 3700 San Martin Drive, Baltimore, MD 21218, USA;
villaver@stsci.edu*

Letizia Stanghellini²

*National Optical Astronomy Observatory, 950 N. Cherry Av., Tucson, AZ 85719, USA;
lstanghellini@noao.edu*

ABSTRACT

The stellar population stripped from galaxies in clusters evolve under the extreme conditions imposed by the intracluster (IC) medium. Intracluster stars generally suffer very high systemic velocities, and evolve within a rarefied and extremely hot IC medium. We present numerical simulations which aim to explore the evolution and survival of IC Asymptotic Giant Branch (AGB) envelopes and Planetary Nebula (PN) shells. Our models reflect the evolution of a low-mass star under the observed conditions in the Virgo IC medium. We find that the integrated hydrogen-recombination line emission of a PN is dominated by the inner dense shell, whose evolution is unaffected by the environment. Ram pressure stripping affects mainly the outermost IC PN shell, which hardly influences the emission when the PN is observed as a point source. More importantly, we find that a PN with progenitor mass of $1M_{\odot}$ fades to $\sim 30\%$ and $\sim 10\%$ of its maximum emission, in 5 000 and 10 000 yr respectively, disclosing an actual PN lifetime (t_{PN}) several times shorter to what is usually adopted (25 000 yr). This result affects the theoretical calculation of the luminosity-specific density of IC PNe, which scales with t_{PN} . For $t_{PN}=10\,000$ yr, our more conservative estimate, we obtain that the luminosity-specific density of PNe is in fair agreement with the value obtained from Red Giants. With our more realistic PN lifetime we infer a higher fraction (above 15%) of IC starlight in the Virgo core than current estimates.

²Affiliated with the Hubble Space Telescope Division of the European Space Agency

³On leave from INAF-Bologna Observatory

Subject headings: Galaxies: Clusters: General, Galaxies: Clusters: Individual:
Name: Virgo, Galaxies: Interactions, Hydrodynamics, ISM: Planetary Nebulae:
General, Shock Waves stars: AGB and post-AGB, Winds, Outflows

1. INTRODUCTION

In the current paradigm, the formation of large-scale structure in the Universe takes place in a hierarchical mode and galaxy clusters are built through mergers of smaller objects. In this scenario, galaxies in clusters undergo fast encounters (“galaxy harassment”, Moore et al. 1996), and tidal interactions (“tidal stirring”, Mayer et al. 2001) that allow stars to escape the gravitational field of their original galaxy, building a diffuse stellar population in the intracluster (IC) medium (Dressler 1984). The total mass, structure, and kinematics of this stripped stellar component can be used to test the cluster’s dynamical history.

The distribution of IC stars is expected to be either smooth or clumpy depending on when in the cluster’s lifetime the stellar component was removed (Merritt 1984; Richstone & Malumuth 1983). An unrelaxed IC stellar component with significant substructure has been predicted by Napolitano et al. (2003) on the basis of a N-body cosmological simulation of a Virgo-like cluster. More elaborated simulations of the IC stellar component by Murante et al. (2004) and Sommer-Larsen et al. (2005) predict that the fraction of the IC stars removed increases with the cluster mass.

From an observational point of view, the diffuse IC component is estimated both from surface brightness measurements and from the detection of individual IC stars. In the last few years, quantitative estimates of the diffuse IC stellar population have been inferred from the study of Red Giants and Asymptotic Giant Branch (AGB) stars in the Virgo cluster (Ferguson, Tanvir, & von Hippel 1998; Durrell et al. 2002), Planetary Nebulae (PNe) in the Virgo and Fornax clusters and the Leo I group (Mendez, et al. 1997; Feldmeier, Ciardullo, & Jacoby 1998; Feldmeier, Ciardullo, Jacoby, & Durrell 2003; Ciardullo, Jacoby, Feldmeier, & Bartlett 1998; Arnaboldi et al. 1996, 2002, 2003; Castro-Rodríguez et al. 2003), Supernovae (SNe) type Ia in the Virgo cluster (Smith 1981; Gal-Yam, Maoz, & Sharon 2002; Gal-Yam, Maoz, Guhathakurta, & Filippenko 2003), and Novae in the Fornax cluster (Neill et al. 2005).

PNe, typically observed via their bright [O III] $\lambda 5007\text{\AA}$ emission line, are among the most useful tracers of IC light to date (Feldmeier 2003; Arnaboldi 2004). Photometric detection is relatively straightforward through narrow-band filters and their spectroscopic confirmation

is possible using moderate resolution spectra. Observations of PNe in the Virgo cluster allow to estimate that the IC stellar component is $\sim 10\%$ of all stars in the cluster (Arnaboldi et al. 2002, 2003; Feldmeier et al. 2004).

While IC PNe are now widely used as probes of the stellar populations stripped from galaxies, and ultimately used to test the cluster’s dynamical history, their formation, evolution, and mere survival in the IC environment has never been analyzed in detail. The stellar population stripped from galaxies in clusters evolve under the extreme conditions imposed by the IC medium. Typically, the stars have very high systemic velocities (up to 2000 km s^{-1}) moving through a rarefied, extremely hot X-ray emitting IC medium. These extreme conditions might affect the PN formation process as well as their survival.

In this paper we present a first attempt to explore the formation and evolution of PN within the IC environment. The idea is to test how the high systemic velocity of the star and the high thermal pressure conditions of the IC medium affect the evolution of the AGB circumstellar shell and the survival of the PN. The ultimate goal is to understand if what we know about PNe in our and in nearby galaxies can be extrapolated to infer the properties of the PN population stripped from galaxies in clusters. In Section §2 we describe the numerical method and the initial and boundary conditions used in the simulations. In §3 we present our results and the relevance they bear in the IC light studies. Finally, in §4 we summarize our results and draw the conclusions of this study.

2. THE NUMERICAL MODEL: INITIAL AND BOUNDARY CONDITIONS

Our numerical calculation follows the evolution of an AGB star of $1 M_{\odot}$ (Main Sequence mass) through the IC medium (with the conditions observed in the Virgo IC medium) until it produces a PN. The stellar wind changes as we follow the evolution from the early-AGB, before the onset of the first thermal pulse, to the post-AGB phase. The modulations of the mass-loss and wind velocity during the TP-AGB phase have been taken from Vassiliadis & Wood (1993). The PN is formed later, when the ejecta is photoionized and shaped by the fast wind from the hot central star. During the post-AGB phase the evolution of the ionizing radiation field and wind are computed following the stellar evolution in the Hertzsprung–Russell (HR) diagram (from Vassiliadis & Wood 1994). Details of the wind assumptions and gas evolution for different initial configurations can be found in Villaver, García-Segura, & Manchado (2002a) and Villaver, Manchado & García-Segura (2002b).

We assume that the star evolves while moving through the IC medium with a velocity of 1000 km s^{-1} , the typical PN velocity observed in the Virgo IC medium (Arnaboldi et

al. 2004). The IC medium gas was assumed to be homogeneous, with a temperature of $T = 10^7$ K (4.75 keV) (Takano et al. 1989), and a density of $n = 10^{-4}$ cm $^{-3}$ (Fabricant & Gorenstein 1983). We consider that the IC pressure is simply the standard gas thermal pressure, $P = nkT$ (where k is the Boltzmann’s constant).

We follow the evolution of the star through the IC medium using the ZEUS-3D code (version 3.4), developed by M. L. Norman and the Laboratory for Computational Astrophysics (Stone & Norman 1992a,b; Stone, Mihalas, & Norman 1992). This is a fully tested code that solves the equations of hydrodynamics (when the magnetic module is off) in a finite-difference, Eulerian, fully explicit scheme. We use radiative cooling which is made according to the cooling curves of Raymond & Smith (1977), and Dalgarno & McCray (1972) for gas temperatures above 10^4 K, and according to MacDonald & Bailey (1981) for temperatures between 10^2 K and 10^4 K. ZEUS-3D does not include radiation transfer, so we use the approximation implemented by García-Segura & Franco (1996) to derive the location of the ionization front (IF) for arbitrary density distributions (Bodenheimer, Tenorio-Tagle, & Yorke 1979; Franco, Tenorio-Tagle, & Bodenheimer 1989, 1990). The position of the IF is determined by assuming that ionization equilibrium holds at all times, and that the ionization is complete within the ionized sphere and zero outside. We apply this formulation by assuming that the nebula is composed of hydrogen, that it is optically thick in the Lyman continuum, and that the “on the spot” approximation is valid. The unperturbed gas is treated adiabatically. Finally, the photoionized gas is always kept at 10^4 K, thus no cooling curve is applied inside the photoionized region, unless there is a shock.

The computations have been performed in 2D in a spherical polar grid (ρ , θ , and ϕ) by assuming axisymmetry in the ϕ coordinate. The angular θ coordinate in the simulations ranges from 0 to 180° and the physical radial extension is 3 pc which gives us a total grid size of 6×3 pc 2 . We have opted for a medium numerical resolution (400 x 360 zones in the radial and angular coordinates of the grid respectively) to solve the problem.

In order to maintain all the details of the wind modulations suffered by the star we have imposed an additional restriction to the Courant-Friedrichs-Levi condition to avoid the timestep of the computation being larger than the timestep of stellar evolution.

We set the time-dependent wind parameters (velocity, mass-loss rate, and wind temperature) within a small spherical region (five radial zones) centered on the symmetry axis where we used a reflecting boundary condition. The density, velocity (normal and tangential components) and energy of the IC medium are updated at each timestep to reflect the inflow that takes place in the angular coordinate from 0 to 90° , and the outflow from 90 to 180° . As similar approach has been used in Villaver, García-Segura, & Manchado (2003) to study the evolution of a slowly moving star in the Galaxy.

3. RESULTS

3.1. The Gas Evolution

The models cover an evolutionary time of 5.3×10^5 yr, 93% of which is spent on the TP-AGB phase. The computation starts at the onset of the TP-AGB phase and is followed until the PN is 30 000 yr old. The zero age for the PN phase is set when the star reaches a temperature of 10 000 K and thus emits a non-negligible amount of ionizing photons. A transition time of 13 000 yr between the AGB and the PN phase has also been included in the simulations. During the transition time we have assumed that the effective temperature of the star increases linearly from the value at the tip of the AGB to 10 000 K, which represents the starting temperature of the post-AGB evolution. Note that we are implicitly assuming that the removal of the star from the parent galaxy had happened in the 10^{10} yr before the star reaches the TP-AGB.

In Figure 1 we show snapshots of the gas density (logarithm scale) at different stages during the AGB evolution of the star. The star is fixed at the center of the grid and the IC medium flows from top to bottom. The computational grid has been projected over the θ axis for illustration purposes. The first snapshot in the top left panel of Fig 1 represents the gas density at 2.8×10^5 yr from the start of the TP-AGB evolution. The subsequent plots (from top to bottom, left to right) show the evolution at time intervals of 24 000 yr, with the exception of the last 3 plots chosen at time intervals of 12 000 yr.

Prior to the so-called superwind phase (Renzini 1981), during the early TP-AGB (the first $\sim 2.2 \times 10^5$ yr) the stellar mass-loss rate and velocity are small and constant with typical values of a Red Giant wind ($10^{-8} M_{\odot} \text{ yr}^{-1}$ and 2 km s^{-1} respectively). Note that this is before the first snapshot shown in Fig. 1. Ram pressure balance is reached very close to the position of the star in the direction of the motion. The stagnation radius (the radius at which pressure balance is reached for a free-streaming wind) is 0.025 pc, and a long stream of gas is generated in the opposite direction to the motion. After this early stage, the mass-loss rate and wind velocity are changing continuously at the inner boundary as the star evolves up the TP-AGB. The star undergoes four major thermal pulses of different duration in which the mass-loss rate increases from $10^{-8} M_{\odot} \text{ yr}^{-1}$ to $5.3 \times 10^{-4} M_{\odot} \text{ yr}^{-1}$ and the wind velocity from 2 km s^{-1} to 15 km s^{-1} (for details see Villaver, García-Segura, & Manchado 2002a). At any given time, this continuously evolving wind cannot be used to compute the stagnation radius, because as shocks develop inside the bow-shock cavity formed by the early time-independent wind, the wind cannot be considered to be free-flowing to reach pressure balance with the IC medium. The ram pressure of the IC medium is balanced by the ram pressure of the stellar wind inside the bow-shock cavity, making it a time-dependent problem. Note that the fluid

is supersonic for the relative velocity we are considering ($1\,000\text{ km s}^{-1}$) between the star and the IC medium.

After 2.6×10^5 yr, the star undergoes the first major thermal pulse and a bow-shock grows in size in the upstream direction. This is the bow-shock visible at 2.8×10^5 yr shown in the top left panel of Fig. 1. In the downstream direction, close to the symmetry axis, the flow turns back. Long tongues of gas, consequence of the stripping process, are also visible. Note the turbulent nature of the stripped gas. About 50 000 yr later (third panel from the top left) the second major thermal pulse has already taken place and subsequently the bow-shock feature in the upstream direction grows in size. About 20 000 yr later, an instability develops in the upstream direction of the bow-shock at an opening angle of $\sim 30^\circ$ that breaks the thin shell formed by the bow-shock.

In the lower panels of Fig.1, the density structure show the effects of the increase in the mass-loss rate taking place at the final thermal pulse. The wind at this stage has enough momentum to allow the formation of the external shell that increasingly grows in size. As a consequence of the interaction with the IC medium gas is continuously removed from the external shell. The material left behind by the star generates a long stream of gas that will have a size of the order of 130 pc if dispersion is prevented.

3.2. The Evolution of the PN Line Emission

In order to gauge the observational differences between a PN evolving in the IC medium and one within a galaxy we have computed the evolution of their $H\alpha$ emission. Note that for the galactic PNe models we refer to models in which there is no relative motion between the star and its surrounding medium. In Figure 2 we show the evolution of the integrated $H\alpha$ emission for the IC (dots) and a galactic (solid line, from Villaver 2001) nebulae, each normalized to its own emission maximum. The dashed line represents a galactic model without transition time evolution (Villaver, Manchado & García-Segura 2002b). The $H\alpha$ intensity in each case has been computed by integrating the $H\alpha$ emission coefficient over nebular volume, assuming an electron temperature of 10 000 K, and case B for the recombination (Osterbrock 1989).

As shown in Fig. 2 the $H\alpha$ line emission decreases very rapidly in both the IC and galactic models. The IC PN emission fades to $\sim 30\%$ of its maximum in 5 000 yr, and to $\sim 10\%$ of its maximum in 10 000 yr. The evolution of the intensity directly reflects the development of dense regions associated with shocks. The first peak in intensity (solid and dashed lines in Fig. 2) is caused by the propagation of the shock front associated with the

ionization front. The intensity maximum is caused by a combination of two effects: the compression generated in the inner shell as the hot bubble develops when the wind velocity increases as the star evolves toward higher effective temperatures, and the transition from an optically thick to an optically thin nebula.

The differences between the solid and dashed lines in Fig. 2 are due to the evolution during the transition time (the time elapsed between the end of the TP-AGB and the PN ionization). The time at which the $H\alpha$ intensity maximum occurs depends on the density structure encountered by the wind and radiation field during the post-AGB phase. During the transition time, the circumstellar gas structure developed during the AGB is diluted. As a consequence, when no transition time is allowed (dashed line), the ionization and fast wind encounter a denser structure, the propagation velocity of the ionization front is retarded, and the transition from optically thick to an optically thin nebula takes longer. Moreover, both the over-pressure generated by the photoionization and the gas density are higher, preventing the expansion of the hot bubble.

We do not find significant differences in the $H\alpha$ decay intensity between the PN in the IC medium (dots) and the galactic model, at least during the bright portion of their evolution. The PN evolving in the IC medium is undergoing strong ram pressure stripping, occurring mainly in the outer shell. The $H\alpha$ intensity is dominated by the brightness of the main nebular shell, at least in the $\sim 5\,000$ yr after the $H\alpha$ maximum, and thus it is not affected by ram pressure stripping. However, after 15 000 yr, the presence of the outer shell has a significant effect on the emitted intensity, but at this point the PN is already below detectability limits when large distances are involved (as is the case for the IC PNe). It is worth noting that the temporal resolution we have used in the IC PN simulation ($\sim 6\,000$ yr) is much smaller than the one used in the galactic models (~ 250 yr) and thus we cannot follow all the fine details of the $H\alpha$ intensity evolution of the IC PN simulation.

It is usually assumed that the evolution of a PN in the Galaxy and in the IC environment are similar. In this work we confirm the validity of this assumption, at least where the decline of the PN $H\alpha$ intensity is concerned. What we find, however, is that in only 10 000 yr the nebular intensity has dropped by a factor of ten from the value at maximum, similarly for IC and galactic PNe. The number of PN in a given stellar population is usually computed assuming that the PN lifetime is $\sim 25\,000$ yr (Mendez et al. 1993; Feldmeier 2003; Aguerri et al. 2005). The effects of a shorter PN lifetime are discussed in §3.3.

The physical reason why the bright PN stage is shorter in our calculation than what is typically assumed can be easily illustrated by simple reasoning. Generally, it is assumed that the hydrogen recombination luminosity is nearly proportional to the number of ionizing photons, a sensible assumption in a constant density regime. Our model reproduce a more

realistic structure that takes into account the hydrodynamic evolution of the gas. Since $I_{H\alpha} \propto \int_V n_e n_p dV$ (where n_e and n_p represent the number density of electrons and protons respectively), the bulk of the recombination line intensity is completely dominated by the PN regions where the density is higher, such as the regions associated with shock fronts. The IC PN, at least under the conditions explored for the Virgo cluster, have a similar fading time as models computed under typical ISM conditions for a galaxy, because the inner shell is not affected by ram pressure stripping. A much higher ram pressure would be required to change the evolution of the bright PN shell.

Note that the logarithmic transformation of the intensity fading is similar to the functional shape of the PN luminosity function (PNLF), and that a factor of ten decrease in intensity translates into an increase of 2.5 magnitudes.

The PN detections in the IC medium are based on the flux measured on the collisionally excited [O III] 5007 Å line. Since we do not solve radiation transfer, we cannot describe the evolution of the [O III] 5007 Å line intensity from our simulations. However, we expect the evolution of the [O III] 5007 Å line and H α to be similar, except in the case of very low metallicity (Stanghellini et al. 2003).

3.3. The IC PN Lifetime and its Implications on the IC Starlight

If, as our simulations suggest, the PN lifetime is indeed shorter than usually adopted, the derived fraction of IC starlight contributing to the total cluster luminosity should be revised.

In order to predict the number of PNe in a given environment we can refer to the fuel consumption theorem (Renzini & Buzzoni 1986), which states that the number of post-main sequence (PMS) stars in a simple stellar population (SSP) is proportional to the population luminosity and to the time elapsed in that particular PMS phase. Obviously, this theorem can be extended to PNe if we rewrite it for the central star (CS) phase of stellar evolution. By definition, $t_{CS}=t_{PN}$, thus, $N_{PN} = B L_T t_{PN}$, where B is the evolutionary flux per unit luminosity of the parent population and L_T is the total bolometric luminosity of the sampled population. Our model has a turnoff mass of $1 M_{\odot}$, thus $B \approx 2 \times 10^{-11}$ PN yr $^{-1}$ L $_{\odot}^{-1}$ (Maraston 1998). The theoretical luminosity-specific PN density can be expressed as $\alpha=N_{PN}/L_T$. If we assume that $t_{PN}=10\,000$ yr we find $\alpha=2.0 \times 10^{-7}$ PN L $_{\odot}^{-1}$, while the luminosity-specific population of the bright 2.5 magnitude bins in the PNLF is about one tenth of this value, if we assume that the PNLF has the shape given by Feldmeier, Ciardullo, & Jacoby (1998). Our value of $\alpha_{2.5}=2 \times 10^{-8}$ PN L $_{\odot}^{-1}$ agrees with the observed value obtained

from IC red giants (Durrell et al. 2002).

In order to assess the effect of our IC PN lifetime estimate, we evaluate the luminosity-specific PN density in the brightest 1.0 magnitude bin of the PNLF, as used by Aguerri et al. (2005). From our lifetime estimate we find that $\alpha_{1.0}$ is between 2.4 and 4.8×10^{-9} PN L_{\odot}^{-1} depending on whether we assume that the IC PN fades in 5 000 or 10 000 yr. For the longer fading time the stars in the Virgo core IC contribute about 7% to the total starlight, as derived by Aguerri et al. (2005) using $\alpha_{1.0}$ from Durrell et al. (2002). We are inclined to believe that a better estimate of the duration of the IC PN life is 5 000 yr, thus the fraction of the IC starlight in the Virgo core would rise to $\sim 15\%$ of the total starlight.

4. CONCLUSIONS

PNe have proved to be among the most useful tracers of IC light to date. Nonetheless, no attempt has been made to date to explore the effects of the IC environment on their evolution. We have simulated the evolution of a $1 M_{\odot}$ star during the AGB and post-AGB phases, as it moves with the typical velocity of 1000 km s^{-1} as is observed in the Virgo IC medium. We found that the evolution of such a star in the IC medium is different from a galactic model in the details of the outer shell structure, but they have similar observable properties when studied as point sources. We based this conclusion on the hydrogen-recombination integrated line emission, and, ultimately, on the fact that the emission is dominated by the bright, inner shell of the PN, which evolves similarly in the IC and galactic cases because it does not get affected by ram pressure stripping until very late in the PN evolution.

These results, while valid to describe the evolution of a PNe in the rarefied IC medium, are not adequate to describe a fast moving star through a much higher density environment, such as that of the Leo I cloud, where no IC PNe have been found (Castro-Rodríguez et al. 2003). We believe that a higher ram pressure might remove more material from the inner PN shell, reducing the IC PN lifetime much further, thus preventing IC PN detection.

We have shown that the PN lifetime is shorter than usually assumed, and we believe that this apply to most IC and galactic environments. In the case under study, the $1 M_{\odot}$ star represent the turnoff mass of a SSP approximately 10 Gyr, and a fading time of 5 000 yr to 10 000 yr is appropriate to theoretically predict the number of PNe per total luminosity. We derived that $\alpha_{2.5} = 2 \times 10^{-8}$ PN L_{\odot}^{-1} , which is in good agreement with the observations of AGB stars. By using our value for $\alpha_{2.5}$ we inferred that the fraction of IC starlight to the total stellar luminosity derived by Aguerri et al. (2005) and Feldmeier et al. (2004) are lower limits. We estimate that the fraction of IC stellar light is greater than 10% of the total

stellar luminosity for a SSP which is 10 Gyr old.

We thank M. L. Norman and the Laboratory for Computational Astrophysics for the use of ZEUS-3D.

REFERENCES

- Aguerri, J. A. L., Gerhard, O. E., Arnaboldi, M., Napolitano, N. R., Castro-Rodriguez, N., & Freeman, K. C. 2005, *AJ*, 129, 2585
- Arnaboldi, M. 2004, *IAU Symposium*, 217, 5
- Arnaboldi, M., Freeman, K. C., Mendez, R. H., et al. 1996, *ApJ*, 472, 145
- Arnaboldi, M., Gerhard, O., Aguerri, J. A. L., Freeman, K. C., Napolitano, N. R., Okamura, S., & Yasuda, N. 2004, *ApJ*, 614, L33
- Arnaboldi, M., et al. 2002, *AJ*, 123, 760
- Arnaboldi, M., et al. 2003, *AJ*, 125, 514
- Bahcall, N. A., Cen, R., Dav, R., Ostriker, J. P., & Yu, Q. 2000, *ApJ*, 541, 1
- Bodenheimer, G., Tenorio-Tagle, G., & Yorke, H. W. 1979, *ApJ*, 233, 85
- Buzzoni, A. 1989, *ApJS*, 71, 817
- Carlberg, R. G., Yee, H. K. C., Ellingson, E., et al. 1996, *ApJ*, 462, 32
- Castro-Rodríguez, N., Aguerri, J. A. L., Arnaboldi, M., Gerhard, O., Freeman, K. C., Napolitano, N. R., & Capaccioli, M. 2003, *A&A*, 405, 803
- Ciardullo, R., Jacoby, G. H., Feldmeier, J. J., & Bartlett, R. E. 1998, *ApJ*, 492, 62
- Dalgarno, A. & McCray, R.A. 1972, *ARA&A*, 10, 375
- Dressler, A. 1984, *ARA&A*, 22, 185
- Durrell, P. R., Ciardullo, R., Feldmeier, J. J., Jacoby, G. H., & Sigurdsson, S. 2002, *ApJ*, 570, 119
- Fabricant, D., & Gorenstein, P. 1983, *ApJ*, 267, 535

- Feldmeier, J. J. 2003, IAU Symposium, 209, 597
- Feldmeier, J. J., Ciardullo, R., & Jacoby, G. H. 1998, ApJ, 503, 109
- Feldmeier, J. J., Ciardullo, R., Jacoby, G. H., & Durrell, P. R. 2003, ApJS, 145, 65
- Feldmeier, J. J., Ciardullo, R., Jacoby, G. H., & Durrell, P. R. 2004, ApJ, 615, 196
- Ferguson, H. C., Tanvir, N. R., & von Hippel, T. 1998, Nature, 391, 461
- Franco, J., Tenorio-Tagle, G., & Bodenheimer, P. 1989, Rev. Mexicana Astron. Astrofis., 18, 65
- Franco, J., Tenorio-Tagle, G., & Bodenheimer, P. 1990, ApJ, 349, 126
- Gal-Yam, A., Maoz, D., Guhathakurta, P., & Filippenko, A. V. 2003, AJ, 125, 1087
- Gal-Yam, A., Maoz, D., & Sharon, K. 2002, MNRAS, 332, 37
- García-Segura, G. & Franco, J. 1996, ApJ, 469, 171
- MacDonald, J. & Bailey, M. E. 1981, MNRAS, 197, 995
- Maraston, C. 1998, MNRAS, 300, 872
- Mayer, L., Governato, F., Colpi, M., Moore, B., Quinn, T., Wadsley, J., Stadel, J., & Lake, G. 2001, ApJ, 547, L123
- Mendez, R. H., Guerrero, M. A., Freeman, K. C., et al. 1997, ApJ, 491, L23
- Mendez, R. H., Kudritzki, R. P., Ciardullo, R., & Jacoby, G. H. 1993, A&A, 275, 534
- Merritt, D. 1984, ApJ, 276, 26
- Moore, B., Katz, N., Lake, G., Dressler, A., & Oemler, A. 1996, Nature, 379, 613
- Murante, G., et al. 2004, ApJ, 607, L83
- Napolitano, N. R., et al. 2003, ApJ, 594, 172
- Neill, J. D., Shara, M. M., & Oegerle, W. R. 2005, ApJ, 618, 692
- Osterbrock, D. E. 1989, Research supported by the University of California, John Simon Guggenheim Memorial Foundation, University of Minnesota, et al. Mill Valley, CA, University Science Books, 1989

- Raymond, J.C. & Smith, B.W. 1977, *ApJS*, 35, 419
- Renzini, A. 1981 in *Physical Processes in Red Giants*, ed.. I. Iben & A. Renzini(Dordrech:Reidel), 431
- Renzini, A., & Buzzoni, A. 1986, *ASSL Vol. 122: Spectral Evolution of Galaxies*, 195
- Richstone, D. O., & Malumuth, E. M. 1983, *ApJ*, 268, 30
- Smith, H. A. 1981, *AJ*, 86, 998
- Sommer-Larsen, J., Romeo, A. D., & Portinari, L. 2005, *MNRAS*, 357, 478
- Stanghellini, L., Shaw, R. A., Balick, B., Mutchler, M., Blades, J. C., & Villaver, E. 2003, *ApJ*, 596, 997
- Stone, J.M., Mihalas, D., & Norman, M. L. 1992, *ApJS*, 80, 819
- Stone, J.M. & Norman, M. L. 1992a, *ApJS*, 80, 753
- Stone, J.M. & Norman, M. L. 1992b, *ApJS*, 80, 791
- Takano, S., Awaki, H., Koyama, K., Kunieda, H., & Tawara, Y. 1989, *Nature*, 340, 289
- Vassiliadis, E. & Wood, P. 1993, *ApJ*, 413, 641
- Vassiliadis, E. & Wood, P. 1994, *ApJ*, 92, 125
- Villaver, E. 2001, Ph.D. Thesis, University of La Laguna
- Villaver, E., García-Segura, G., & Manchado, A. 2002a, *ApJ*, 571, 880
- Villaver, E., García-Segura, G., & Manchado, A. 2003, *ApJ*, 585, L49
- Villaver, E., Manchado, A., & García-Segura, G. 2002b, *ApJ*, 581, 1204

Fig. 1.— Snapshots of the (logarithmic) gas density generated during the AGB evolution of a $1 M_{\odot}$ star moving in the IC medium. We have assumed a relative velocity of 1000 km s^{-1} , with the IC medium flowing into the grid from top to bottom. The evolution of the stellar wind during the thermal-pulsing AGB phase and the PN stage has been implemented at the center of the grid. The star suffers four major thermal pulses at 2.6×10^5 , 3.3×10^5 ,

4.1×10^5 , and 4.8×10^5 yr, each of them with a different duration. From top to bottom and left to right the snapshots have been taken at 2.8×10^5 , 3.0×10^5 , 3.3×10^5 , 3.5×10^5 , 3.8×10^5 , 3.9×10^5 , 4.0×10^5 , and 4.14×10^5 yr respectively.

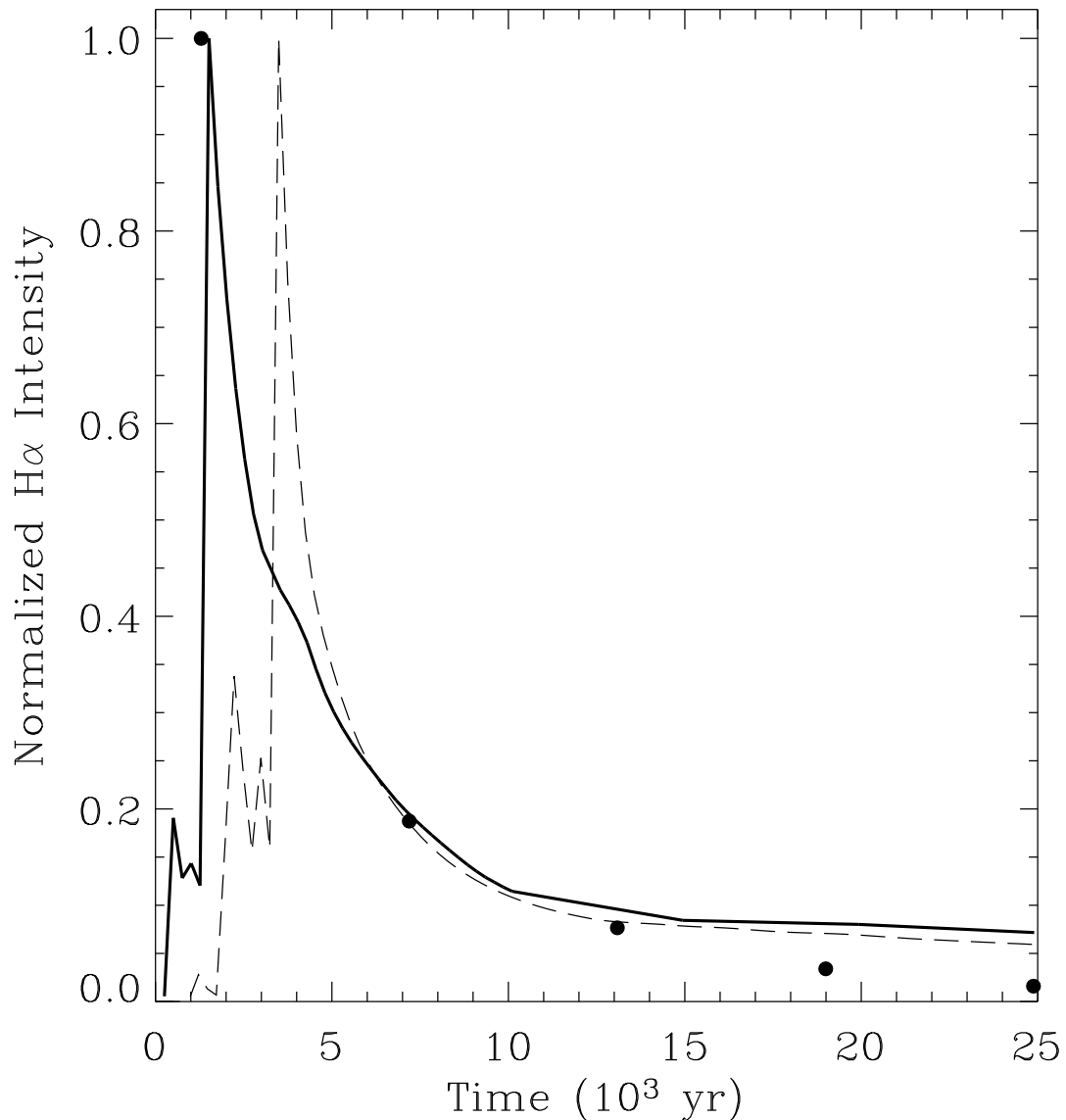


Fig. 2.— The evolution of the total integrated H α intensity emitted by the PNe evolving in the Galaxy (solid line) and the IC medium (dots), normalized to their maxima. In this figure the timescale represent the time elapsed after the PN illumination (i.e., when $T_{\text{eff}}=10\,000$ K). Both PN models (Galaxy and IC medium) include evolution during the transition time (see text). As a comparison, a galactic model without the evolution during the transition time is plotted as a dashed line.

This figure "f1.jpg" is available in "jpg" format from:

<http://arxiv.org/ps/astro-ph/0506612v1>